Research Paper https://doi.org/10.7733/jnfcwt.2024.016

A Comparative Study on Gamma-ray Measurement and MCNP Simulation for Precise Measurement of Spent Nuclear Fuel Burnup

Sohee Cha and Kwangheon Park*
Kyung Hee University, 1732, Deogyeong-daero, Giheung-gu, Yongin-si, Gyeonggi-do 17104, Republic of Korea

(Received January 12, 2024 / Revised January 25, 2024 / Approved April 18, 2024)

To non-destructively determine the burnup of a spent nuclear fuel assembly, it is essential to analyze the nuclear isotopes present in the assembly and detect the neutrons and gamma rays emitted from these isotopes. Specifically, gamma-ray measurement methods can utilize a single radiation measurement value of ^{137}Cs or measure based on the energy peak ratio of Cs isotopes such as ^{134}Cs/^{137}Cs and ^{154}Eu/^{137}Cs. In this study, we validated the extent to which the results of gamma-ray measurements using cadmium zinc telluride (CZT) sensors based on ^{137}Cs could be accurately simulated by implementing identical conditions on MCNP. To simulate measurement scenarios using a lead collimator, we propose equations that represent radiation behavior that reaches the detector by assuming "Direct hit" and "Penetration with attenuation" situations. The results obtained from MCNP confirmed an increase in measurement efficiency by 0.47 times when using the CZT detector, demonstrating the efficacy of the measurement system.

Keywords: Spent nuclear fuel, Burnup, MCNP, CZT, Reaction rate

*Corresponding Author.
Kwangheon Park, Kyung Hee University, E-mail: kpark@khu.ac.kr, Tel: +82-31-201-2563

ORCID
Sohee Cha http://orcid.org/0000-0002-0493-0366 Kwangheon Park http://orcid.org/0000-0003-2477-6674

1. Introduction

The issue of managing high-level radioactive waste is emerging due to the saturation of domestic spent nuclear fuel storage capacity [1]. In February 2023, a briefing organized by the Ministry of Trade, Industry, and Energy revealed that 72,000 assemblies and 722,000 bundles of spent nuclear fuel are expected to be generated. The Hanbit Nuclear Power Plant storage facility is anticipated to reach saturation as early as 2030, followed by sequential saturation of the Hanul Nuclear Power Plant in 2031 and the Gori Nuclear Power Plant in 2032. These saturation points are attributed to the phenomena resulting from nuclear power plant construction and operational plans, as well as the increase in nuclear power utilization rates.

Consequently, there is a pressing need for the establishment of facilities for the disposal of high-level radioactive waste. To address the concerns of residents regarding these facilities, proactive communication and swift enactment of the High-Level Radioactive Waste Management Special Act are essential. However, even if these measures are promptly discussed, agreed upon, and legislated, a considerable amount of time will be required for site selection, disposal facility construction, and operation.

Therefore, it is inevitable to operate dry storage facilities temporarily to alleviate saturation. Dry storage facilities involve removing spent nuclear fuel from wet storage tanks and storing it aboveground. Accurate radiation measurement and analysis technologies are crucial to ensure the safe management, transportation, and storage of spent nuclear fuel [2-4]. The constituents of spent nuclear fuel include fertile materials, trans-uranium material, and fission products [5]. Particularly, gamma radiation can measure the burnup of spent nuclear fuel, with ^{137}Cs being dominantly influenced by this process [6-8].

In this study, we confirmed the extent to which results from gamma radiation measurement experiments using CZT sensors could be reflected by simulating identical conditions on MCNP.

2. Materials and Methods

2.1 Selection of Gamma-ray Detector: CZT

A CZT (Cadmium Zinc Telluride) semiconductor detector was selected to measure the energy and dose of gamma-rays generated in the fuel assembly. The device accepts

Table 1. Specification for CZT

Detector sensitive volume	500 mm^2	
Performance (at operation temperature +22℃)		
Energy resolution (FWHM) at 662 keV line	For CZT/500	≤ 30 keV
	For CZT/500S	≤ 18 keV
Peak-to-Compton ratio at 662 keV line	For CZT/500	≤ 2.3
	For CZT/500S	≤ 4.0
Bias voltage requirements		
Detector high voltage	≤ 1,500 V	
Detector high voltage polarity	Positive	
Dimensions		
Diameter	23 mm	
Length (without connector)	33 mm	
Distance between the top plane of the housing cover and the sensitive surface	7 mm	

Fig. 1. CZT/500S detector.

gamma-rays in the direction of a CdZnTe single crystal.

The CZT detection unit was selected based on the quasi-hemispherical geometry of 'CZT/500S (Ritec SIA)'. The CdZnTe single crystal receiving the signal is 10 × 10 × 5 mm, with a detection area of 500 mm^3, and operates at a drive voltage of 1,500 V or below. In subsequent actual experiments involving CZT, the detection unit's single crystal will be simulated to concentrate gamma-rays towards it, with the device enclosed in lead shielding to minimize the impact from gamma-rays.

2.2 Comparison of Gamma-ray Measurement Experiment and MCNP Simulation

The correctness of the calculations was verified by comparing the results of the gamma-ray measurement experiment with those obtained from the MCNP simulation. The energy spectrum was evaluated using standard radiation sources (85 μCi, Eckert & Ziegler) of representative gamma-emitting isotopes, ^{134}Cs, and ^{137}Cs, generated from spent nuclear fuel. Gamma rays were emitted at a rate of approximately 3.145 × 10^6 per second, considering an emission probability of 94.6%, resulting in an effective emission rate of 2.97517 × 10^6 per second. A lead collimator was positioned between the radiation source and the CZT detector to ensure parallel incidence of incoming particles.

By examining the gamma-ray dose based on the thickness (3, 4 cm) and inner diameter (1–4 mm) of the lead collimator, results similar to those shown in Fig. 3 can be

Fig. 2. Gamma-ray measurement experiment with lead shielding.

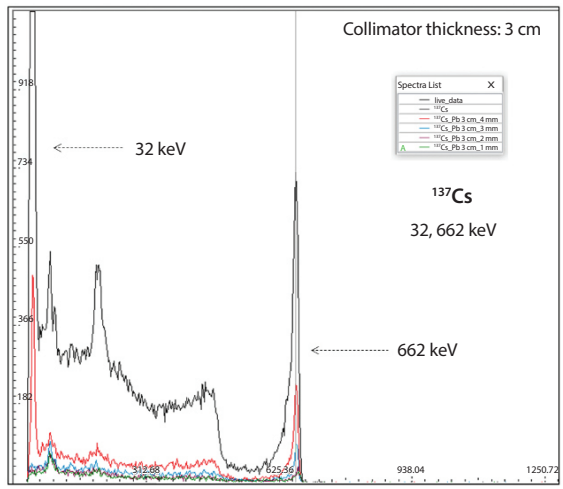

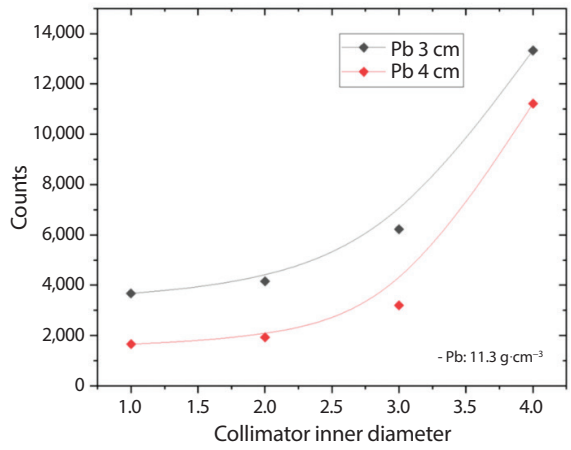

Fig. 3. Energy spectrum measured by CZT detector with lead shielding (3 cm) for ^{137}Cs (left: pin hole 1–4 mm), ^{252}Cf (right: Pb 3, 4 cm).

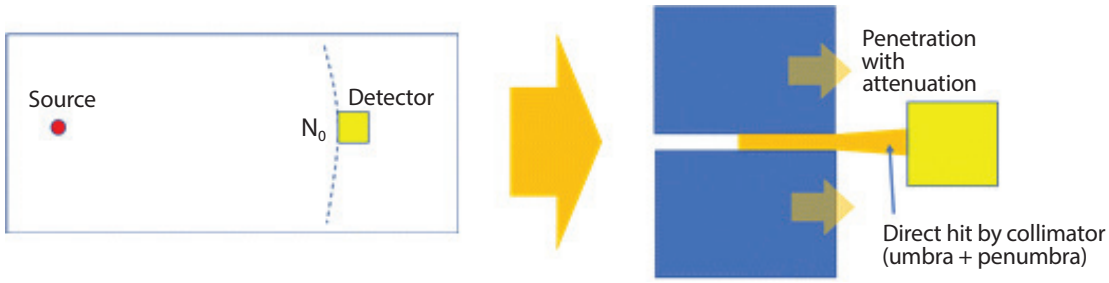

Fig. 4. Particle colliding head-on with the collimator (direct hit).

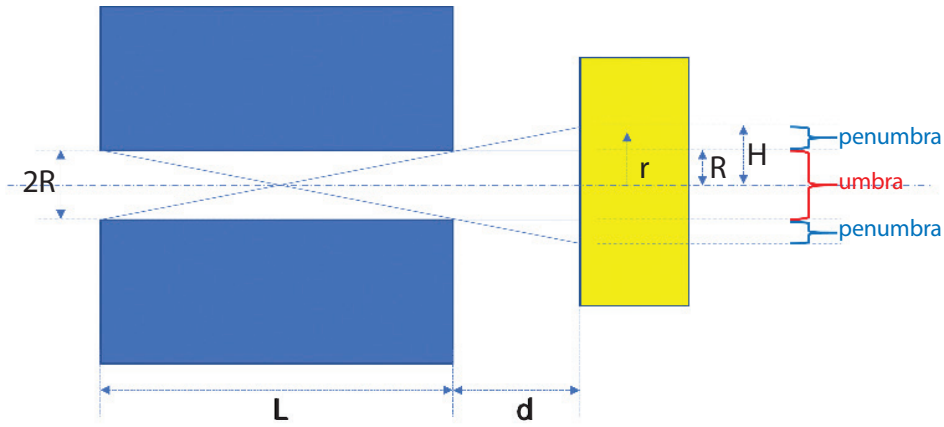

Fig. 5. Umbra and penumbra.

obtained [8]. The thickness of the collimator must be carefully determined to accurately measure the gamma dose of ^{137}Cs, which is the main nuclide of burnup measurement. The attenuation rate was about 84% compared to before the application of the collimator at the thickness of 4 cm and the inner diameter of 4 mm, and the main peak of 662 keV was confirmed while the attenuation rate was about 98% at the thickness of 4 cm and the inner diameter of 1 mm [9]. Therefore, accurate gamma dose measurement is possible if a gamma-ray measurement system is configured using the corresponding thickness and inner diameter.

However, it should be noted that there is an experimental limitation as the shielding configuration was not separately designed for the space surrounding the radiation source, excluding the inner diameter of the collimator. Consequently, there is a possibility of gamma-rays incident from directions other than the straight-line distance being detected during measurement.

3. Evaluation of Gamma-ray Attenuation Rate

Before implementing the conditions of this experiment in the MCNP simulation, the phenomenon of radiation being detected by the collimator was modeled using mathematical expressions.

3.1 Pb Plate With a Collimeter (hole) Modeling: Direct Hit

When radiation reaches an object, the central line

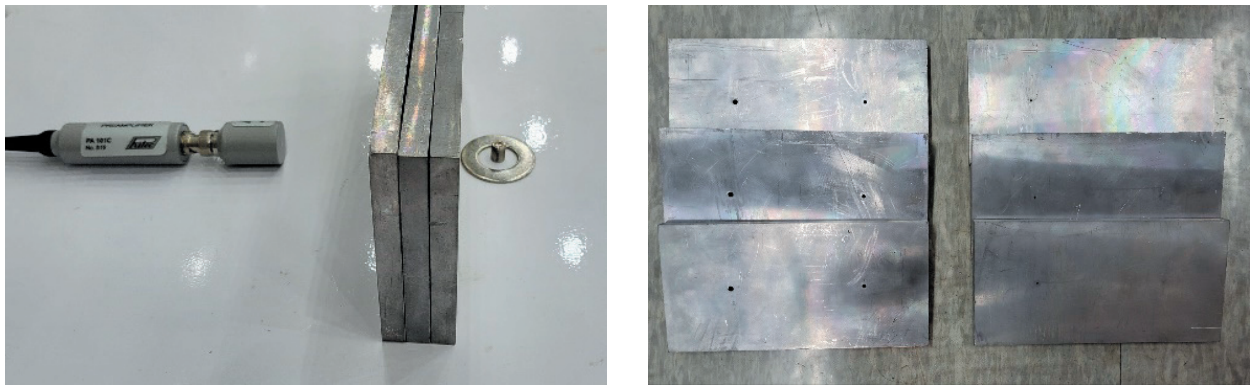

Fig. 6. CZT Gamma-ray experiment (left) and lead collimator (right).

reaching perpendicularly and its corresponding shadow are respectively termed 'Umbra' and 'Penumbra' (Fig. 4). The initial radiation is assumed to be N_0. If f(r) represents a function for radiation within the penumbra, it can be expressed by the following Equation (1).

$$N = Direct\ hit + Penetration$$

$$f(r) = N_0 + \frac{H-r}{H-R} \tag{1}$$

Where f(r): radiation flux at penumbra area, N_0 at r = R, 0 at r = H

Therefore, the radiation N reaching through a direct hit collision can be expressed as follows.

$$N = \pi R^2 N_0 + \int_R^H f(r) 2\pi r\, dr \tag{2}$$

The combined region H of the umbra and penumbra obtained through direct hit can be expressed as shown in the equation.

$$H = \frac{2R}{L}(L+d) - R = \left(1 + \frac{d}{L}\right)R \quad \text{or,}$$

$$\frac{H}{R} = 1 + \frac{d}{L} = 1 + q \tag{3}$$

where $q = \frac{d}{L}$

When determining the radiation N reaching, it can be formulated as in Equation (4).

$$N = \pi R^2 N_0 + N_0 \int_R^H \frac{H-r}{H-R} 2\pi r\, dr$$

$$= \pi R^2 N_0 + \frac{2\pi}{H-R} N_0 \int_R^H (H-r) r\, dr \tag{4}$$

Simplifying Equation (4), the final expression for a direct hit can be presented as follows.

$$N = \pi R^2 N_0 \left(1 + \frac{1}{3}\frac{d}{L}\left(\frac{d}{L} + 3\right)\right) \quad \text{or,}$$

$$N = \pi R^2 N_0 \left(1 + \frac{1}{3} q(q+3)\right) \tag{5}$$

3.2 Penetration With Attenuation

Secondly, consideration was given to the phenomenon of radiation encountering lead shielding and undergoing attenuation. Radiation interacts with the medium as it passes through, losing energy, a process referred to as attenuation. Assuming the initial radiation is N_0, the remaining energy after passing through the shielding is expressed as follows.

$$N = N_0\, e^{-\mu x} \tag{6}$$

Where N = intensity after attenuation

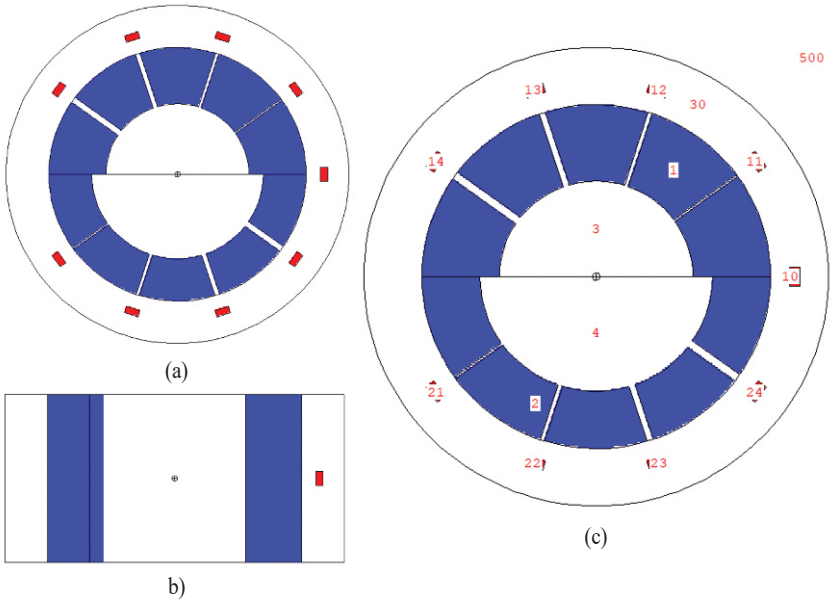

Fig. 7. CZT detector modeling in cylindrical concept (a) upper face, (b) lateral face, (c) upper face with cell number.

Table 2. Cell number and corresponding notations

Cell	Notation	Cell	Notation	Cell	Notation
11	4 cm 1 mm	21	3 cm 1 mm	25	3 cm 0 mm
12	4 cm 2 mm	22	3 cm 2 mm	26	4 cm 0 mm
13	4 cm 3mm	23	3 cm 3 mm	10	5 cm 0 mm
14	4 cm 4 mm	24	3 cm 4 mm		

N_0 = incident intensity
μ = linear attenuation coefficient (cm^{-1})
L = thickness of the absorber

Considering both Equations (5) and (6), the radiation reaching the detector after passing through the lead collimator can be expressed by the following Equation (7). This formula can be used for comparative verification to derive clearer values when trying to obtain experimental values using collimators.

$$N_{tot} = N_D + N_P = \pi R^2 N_0 \left(1 + \frac{1}{3} q(q+3)\right) + N_0 e^{-\frac{\mu}{\rho}\rho L} \quad (7)$$

Gamma-ray measurement experiments were conducted as depicted in the left image of Fig. 6. A collimator made of lead was positioned between the radiation source and the CZT sensor, and measurements were obtained. Collimator thicknesses of 3 cm and 4 cm were prepared, and holes ranging from 1 to 4 mm were drilled, taking into account the possibility of variations in gamma-ray intensity based on the inner diameter.

4. Geometry Modeling in Cylindrical Concepts and Corresponding Result

To check the results for various thicknesses and hole inner diameters at once, it was simulated as shown in Fig. 7

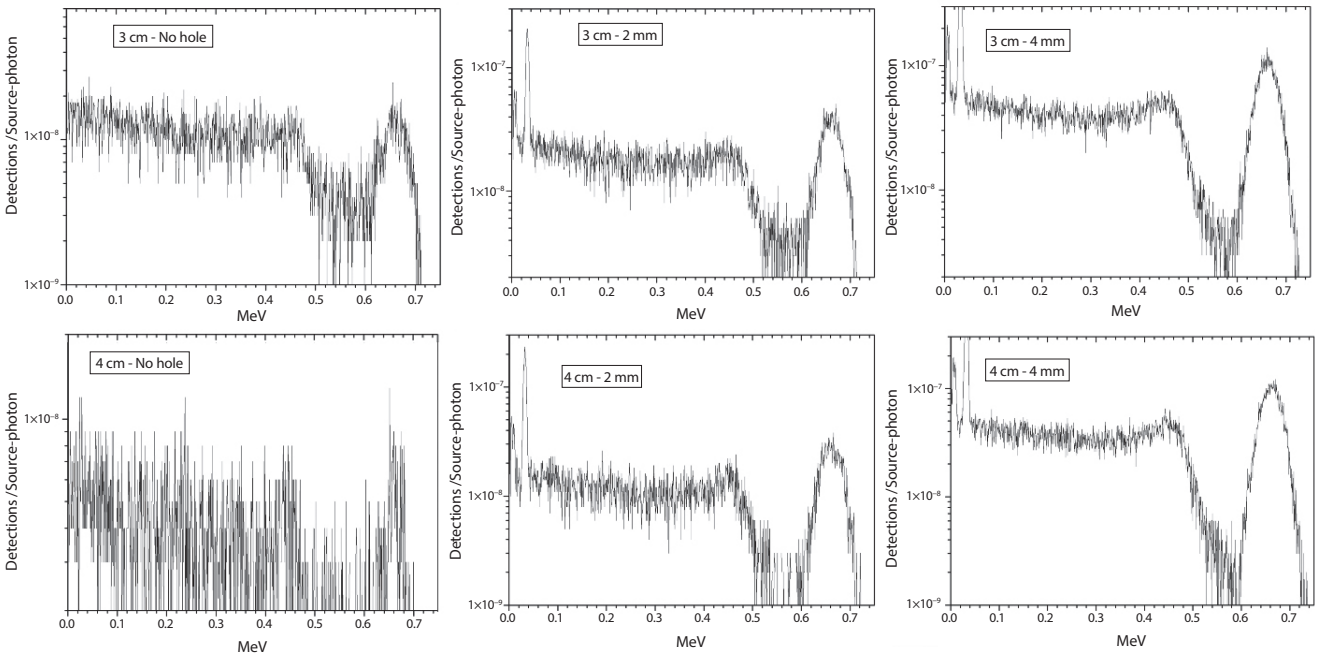

Fig. 8. Energy spectrum results with GEB.

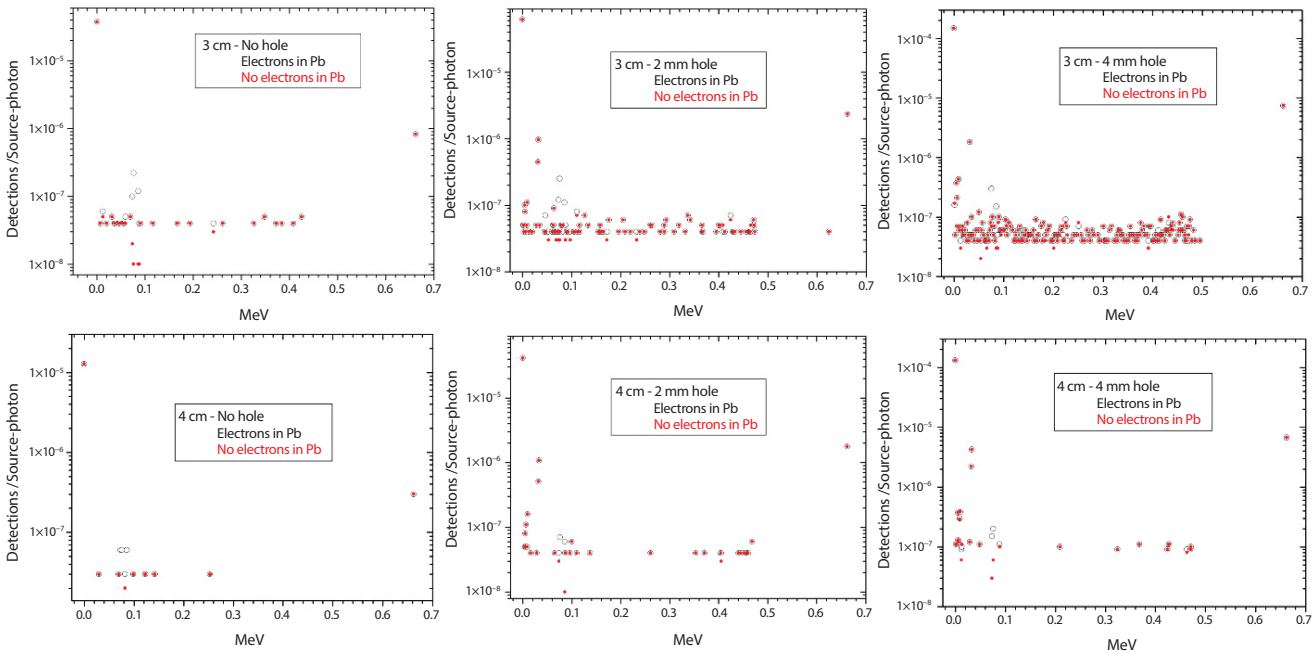

Fig. 9. Energy spectrum results with no GEB.

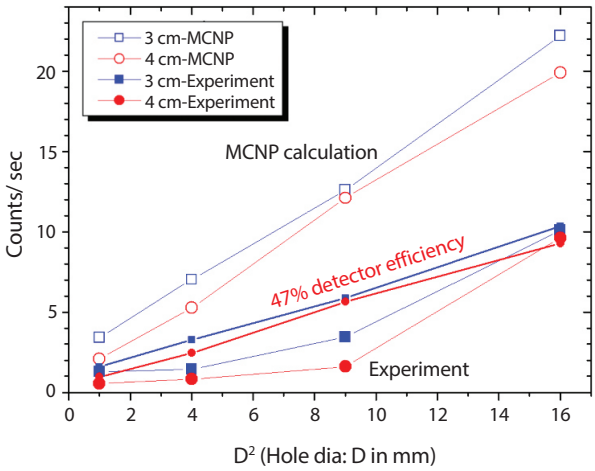

Fig. 10. Efficiency comparison between gamma-ray measurement values and MCNP results.

through MCNP. Table 2 shows the information of each cell.

F8 tally and 1,000 channels of energy bin cards were used to calculate the energy spectrum for particles p and e. The energy band for peak observation of ^{137}Cs was set to 10^{-5} to 0.8 MeV. Nps was set to 1e8. In addition, in order to obtain a result similar to the actual spectrum, Gaussian Energy Broadcasting (GEB) was set, and a result value was derived when GEB was not set. Figs. 8 and 9 below show some of the result values.

Comparing the actual experimental results in Fig. 3 with the corresponding results, the main areas such as the total energy peak from the interaction between gamma rays and the detector are well illustrated across the energy spectrum. Fig. 9, which is the result of not applying GEB, simulates the result more simply.

After simulating the experimental environment using MCNP, focusing on significant results with 3 mm and 4 mm collimators, the outcomes were confirmed as illustrated in Fig. 10.

Using the 0.662 MeV peak as a reference, the MCNP results were 0.47 times the CZT measurement values, indicating an efficiency of 47% for each peak coefficient efficiency concerning the MCNP results. Therefore, the correlation between the actual measurement values and MCNP can be expressed by the following equation.

For the peak coefficient efficiency,

$$Det.\ Peak\ Counts = MCNP\ react. \times 0.47 \quad (8)$$

Det. = Detection value
react. = Reaction rate (reactions/cell)

When the reaction rate value is known by scanning the spent nuclear fuel using the non-destructive testing method through the gamma-ray measuring instrument, the reliability can be determined by comparing the value with the simulated MCNP value. Thus, applying the efficiency corresponding to Equation (8) to the reaction rates calculated by MCNP, a correlation equation for gamma-ray measurements can be established.

5. Conclusion

Utilizing this study, it is possible to predict the burnup of spent nuclear fuel from gamma-ray detector measurements based on the gamma-ray reaction rate. In the earlier comparison between gamma-ray measurement experiments and MCNP simulations, the MCNP results were 0.47 times the measured values using the 0.662 MeV peak counts as a reference.

Converting the values to weight per 1 MTU (Det. Total Counts or Det. Peak Counts), multiplying by the efficiency of 0.47 as indicated in Equation (8), and applying the resulting value to the total neutron reaction rate (RR) calculated by MCNP, we can predict the burnup of spent nuclear fuel by applying the RR value at that moment to the function in Equation (9).

With the MCNP results serving as a reference, the detector efficiency is indicated to be 47% concerning the peak counts. Therefore, if the value converted to weight per 1 MTU (Det. Total Counts or Det. Peak Counts) matches

the value calculated by MCNP for the total neutron reaction rate (RR), multiplied by the corresponding efficiency of 0.47 as expressed in Equation (8), then applying the RR value at that moment to the function in Equation (9) enables the prediction of the burnup of spent nuclear fuel [10].

$$BU = f(RR, IE, CT, x) \quad (9)$$

Therefore, by applying the gamma-ray reaction rate (RR) calculated by MCNP to the measured values obtained by the CZT gamma-ray detector, it is possible to predict the burnup of spent nuclear fuel using the method illustrated in Fig. 10.

Conflict of Interest

No potential conflict of interest relevant to this article was reported.

Acknowledgements

This work was partly supported by Korea Institute of Energy Technology Evaluation and Planning (KETEP) grant funded by the Korea government (MOTIE) (20222B10100060, Development of On-site Burn-up Detection System for the Spent Fuel).

REFERENCES

[1] S.H. Cha and K.H. Park, "An Analysis of Neutron Sources and Gamma-Ray in Spent Fuels Using SCALE-ORIGEN-ARP", J. Surf. Sci. Eng., 56(1), 84-93 (in Korean) (2023).

[2] H. Trellue, G. McMath, A. Trahan, A. Favalli, T. Burr, A. Sjöland, and U. Bäckström, "Spent Fuel Nondestructive Assay Integrated Characterization From Active Neutron, Passive Neutron, and Passive Gamma", Nucl. Instrum. Methods Phys. Res. A, 988, 164937 (2021).

[3] C.A. Miller, W.A. Peters, F.Y. Odeh, T.H. Shin, M. Mamtimin, S.D. Clarke, T.L. Grimm, and S.A. Pozzi, "Sub-Critical Assembly Die-Away Analysis With Organic Scintillators", Nucl. Instrum. Methods Phys. Res. A, 959, 163598 (2020).

[4] S.M. Bowman and I.C. Gauld, OrigenArp Primer: How to Perform Isotopic Depletion and Decay Calculations With SCALE/ORIGEN, Oak Ridge National Laboratory, ORNL/TM-2010/43 (2010).

[5] J. Hu, R. McElroy Jr., A.D. Nicholson, and S. Croft. Fork Experiments in the Hot Cell Using Spent Fuel Rods for International Nuclear Safeguards, Oak Ridge National Laboratory Technical Report, ORNL/SPR-2020/1774 (2021).

[6] S. Vaccaro, I.C. Gauld, J. Hu, P. de Baere, J. Peterson, P. Schwalbach, A. Smejkal, A. Tomanin, A. Sjöland, S. Tobin, and D. Wiarda, "Advancing the Fork Detector for Quantitative Spent Nuclear Fuel Verification", Nucl. Instrum. Methods Phys. Res. A, 888, 202-217 (2018).

[7] T.W. Doering and G.A. Cordes, "Status of the Multi-Detector Analysis System (MDAS) and the Fork Detector Research Programs", Proc. of Technical Committee Meeting on Implementation of Burnup Credit in Spent Fuel Management Systems, IAEA-TECDOC-1241, 286-297, IAEA, Vienna (2000).

[8] H.M. Park, T.Y. Kim, Y.S. Song, U.J. Lee, and C.M. Ham, "Spectroscopic Properties of Gamma-Ray Detector to Measure the Burnup of Spent Nuclear Fuel", J. Radiat. Ind., 17(1), 119-125 (in Korean) (2023).

[9] S. Cha, K. Park, M.O. Kim, J.H. Ko, and J.H. Sung, "A Method to Estimate the Burnup Using Initial Enrichment, Cooling Time, Total Neutron Source Intensity and Gamma Source Activities in Spent Fuels", J. Nucl. Fuel Cycle Waste Technol., 21(3), 303-313 (2023).